Electrick: Low-Cost Touch Sensing Using Electric Field Tomography

Yang Zhang   Gierad Laput   Chris Harrison

Human-Computer Interaction Institute, Carnegie Mellon University

5000 Forbes Avenue, Pittsburgh, PA 15213

{yang.zhang, gierad.laput, chris.harrison}@cs.cmu.edu

ABSTRACT

Current touch input technologies are best suited for small and flat applications, such as smartphones, tablets and kiosks. In general, they are too expensive to scale to large surfaces, such as walls and furniture, and cannot provide input on objects having irregular and complex geometries, such as tools and toys. We introduce Electrick, a low-cost and versatile sensing technique that enables touch input on a wide variety of objects and surfaces, whether small or large, flat or irregular. This is achieved by using electric field tomography in concert with an electrically conductive material, which can be easily and cheaply added to objects and surfaces. We show that our technique is compatible with commonplace manufacturing methods, such as spray/brush coating, vacuum forming, and casting/molding – enabling a wide range of possible uses and outputs. Our technique can also bring touch interactivity to rapidly fabricated objects, including those that are laser cut or 3D printed. Through a series of studies and illustrative example uses, we show that Electrick can enable new interactive opportunities on a diverse set of objects and surfaces that were previously static.

Author Keywords

Touch sensing; Finger tracking; Electric Field Sensing; Tomography; Rapid prototyping; Interactivity tools.

ACM Classification Keywords

H.5.2. [User interfaces] – Input devices and strategies.

INTRODUCTION

Today's touchscreen technologies are generally manufactured on a rigid substrate. For example, projective capacitive sensing, like that used in contemporary smartphones, uses a multi-layered, row-column matrix most often deposited onto glass. This means that most touch panels are relatively small and flat. In cases where irregular shapes or large areas have been made touch sensitive, the price tag is often substantial – touchscreens above 75" typically cost thousands of dollars [2, 30], and irregular or flexible objects with touch-sensing capabilities are mostly research prototypes unavailable to consumers [22, 27, 40, 57]. This high cost and inflexibility has limited touch interaction from being adopted by a wider array of everyday objects, despite touch being an intuitive and popular input modality. In response, researchers have long investigated ways to enable touch sensing on new classes of objects [22, 35, 55], including everyday surfaces [10, 39, 40, 58] and rapidly prototyped artifacts [24, 44, 48, 56].

In this paper, we present our work on Electrick, an inexpensive and versatile touch sensing approach, which is applicable to a wide range of objects and surfaces – including those with large, irregular, and even flexible geometries. To enable Electrick, objects must either be made from an electrically conductive material, or have a conductive coating. The latter can be easily and cheaply applied through e.g., painting, allowing for large touch surfaces (e.g., walls, furniture) at under $1 per square foot of interactive area. In total, we identified six commercially available materials that are applicable to a variety of manufacturing processes, including CNC milling, stamping/forming and molding/casting, as well as additive methods, such as FDM 3D printing.

To track a finger's touch location, electrodes are attached to the periphery of the desired interactive area. A sensor board connected to these electrodes injects an electric field into the conductive substrate, and senses changes in the field's distribution resulting from a user's touch. Sensor data can be transmitted wirelessly, allowing the electronics to be fully contained within an object, eliminating the need for external sensing infrastructure (e.g., depth cameras).

Our technique is readily accessible to hobbyists, requiring no special chemicals, equipment or facilities; everything required can be readily purchased online. This allows Electrick to be applied to existing objects and surfaces, augmenting them with new touch sensing capabilities. Of course, such coatings could also be applied during the initial manufacturing process to create new interactive goods at costs compatible with mass production. Finally, as we will show, Electrick can also bring touch interactivity to rapidly prototyped objects (e.g., 3D printed), enabling rapid iteration of both form and function.

RELATED WORK

Electrick intersects with three key literatures. First we review prior work that relates to our core technical approach. We then discuss a broader set of work that overlaps with our application domain: infusing objects and surfaces with touch interactivity. As our technique is also applicable to rapidly prototyped artifacts, we conclude with a more specialized review of literature in this area.

Technical Approach

Our sensing principle is based on the shunting effect, where a human body proximate to an electric field draws a small amount of current to ground. This phenomenon, also called "shunt mode", has been widely utilized in Electric Field (EF) sensing systems [42, 43, 61]. EF sensing generally uses the air as a medium, enabling free-space interactions such as finger tracking [18], motion sensing [13] and activity recognition [33]. By using measurements from peripheral electrodes, it is possible to deduce the position of the shunting object. The combination of EF sensing and tomography was demonstrated in seminal work by Smith [42, 43]. We also employ Electric Field Tomography (EFT), though constrained to a conductive medium.

This shunting effect has also been utilized for many single-touch touchscreens [15, 26]. In this case, the electric field is constrained to a conductive substrate, which requires electrodes attached to the periphery. Though this setup is physically similar to Electrick, these touchscreen techniques use low-conductivity materials (e.g., ITO, PEDOT) and rectilinear sensing areas. This limits these techniques from being used in ad hoc existing objects, as well as fabricated ones. In contrast, Electrick works with a wide range of material resistances (500Ω-50MΩ/sq), and can work on irregular and non-rectangular surfaces, allowing us to use methods and materials compatible across many fabrication processes.

Finally, our measuring scheme is closely related to Electrical Impedance Tomography (EIT). This technique is widely used to reconstruct the interior structure of an object by sensing non-invasively from the exterior surface. Classic EIT applications include respiratory monitoring [49], underground detection [11] and biological inspection [50]. In the HCI domain, we recently adapted the technology for use in a hand-gesture-sensing smartwatch [62, 63].

EIT has been used in conjunction with materials that alter their local impedance when pressure is applied by a finger, such as piezo-resistive films [38], multilayer meshes [9, 51], and tactile sensor arrays [22]. This has been used, most notably, to create touch sensitive skins for robots [9, 22, 51, 52]. Like Electrick, irregular geometries are supported, though no prior work has demonstrated scalability beyond roughly 0.5 m^2. Further, although Electrick also uses tomography, the sensing principles are very different – our method does not sense changes in a material substrate (impedance in the case of EIT), but is rather based on a user's finger shunting current. This different sensing mechanism allows us to leverage different (and low cost) materials for our conductive domain, which in turn enables different fabrication methods and use cases.

Touch Sensing on Everyday Objects and Surfaces

Researchers have developed a myriad of approaches to enable touch-screen-like interactions on ad hoc objects and surfaces, ideally with minimal instrumentation of either the object itself or the environment.

The most prevalent way to achieve this level of fidelity (at scale) is through computer vision. Early systems, such as Light Widgets [17] and PlayAnywhere [55], used conventional cameras segmenting e.g., skin color, motion or shadows. Depth cameras have been a notable boon, easing the previously complex task of segmenting user inputs from a background scene; notable systems include Light Space [54] and WorldKit [58]. It is also possible to super-size touchscreen technologies to room scale; for example, Multi-toe [10] uses an augmented floor with FTIR sensing.

Next most popular are acoustic methods. Multi-sensor approaches, chiefly based on time difference of arrival techniques, can enable touch sensing on large surfaces, including windows, wall and desks [37, 41, 59]. Passive acoustics can also be used to capture and recognize non-spatial gestures [20]. Several of these approaches can be applied to discrete objects. For example, Touch and Activate [35] used an emitter-receiver pair of Piezo-electric elements to recognize touches to discrete locations on ad hoc objects.

Least common are electrical methods. One option, as demonstrated by Cohn et al. [14], is to detect touch locations in an environment by passively capturing ambient electromagnetic noise that couples to users when they are near to a noise source (e.g., a power line behind a wall). Active approaches are also possible. For example, TactileTape [21] is a 1D, capacitive, flexible, touch-sensing tape that can be easily affixed to objects. MaKey MaKey [12] allows users to appropriate conductive objects (e.g., fruits, Play-doh, toys) as capacitive buttons. Touché [39] uses a more advanced swept frequency capacitive sensing approach to enable discrete touch location sensing, continuous 1D tracking and hand-gesture controls.

Finally, it is also possible to create materials with special, integrated features that enable touch capabilities. These are not ad hoc objects *per se*, but rather augmented versions of everyday materials. The most common target for these efforts has been textiles. Through silk-screening or weaving of conductive materials, sensing of discrete touch locations [34] and even multi-touch inputs is possible [40]. Most projects utilize capacitive sensing, though other techniques, such as Time Domain Reflectometry [57], have also been applied with success.

Adding Interactivity to Rapidly Prototyped Objects

The last decade has seen tremendous growth in digitally-augmented, rapid fabrication tools, especially for HCI uses such as prototyping enclosures, controllers, and new computing form factors. However, the outputs from these tools,

such as CNC milling machines, laser cutters, vacuum formers and 3D printers are *static* – output embodies the desired 3D form, but rarely the interactivity of the end product. Ideally, designers should be able to prototype both in the same medium, as eloquently motivated in [24].

A variety of approaches have been considered that aim to alleviate this interactive divide. For example, DisplayObjects [8] detects touch input on passive prototyped objects by tracking fingers using an external camera array. Also using computer vision, Makers' Marks [47] allows users to annotate objects they have created with stickers, which denotes locations of desired functionality (e.g., "joystick here"); after 3D scanning and processing, the final functional object can be 3D printed and assembled by non-experts.

Due to its non-mechanical nature, capacitive sensing is a powerful and popular technique for prototyping or retrofitting touch input. Hudson and Mankoff [24] demonstrate rapid construction of functional physical interfaces using just "cardboard, thumbtacks, tin foil and masking tape". Midas [48] provides an entire workflow for authoring and fabricating complex capacitive layouts (using a CNC vinyl cutter), which can then be adhered to complex objects. The aforementioned capacitive TactileTape [21] can also be used in a prototyping context.

Owing to 3D printing's versatility, a variety of methods have been explored to enable interactive printed output. For example, by 3D printing integrated cavities, tubes, tines and other mechanical structures, active [28] and passive [45] acoustics can be used to capture user input. Sauron [46] uses an internal camera and computer vision, along with accessory mirrors and markers, to digitize user manipulated mechanical controls. It is also possible to 3D print light pipes, which can route optically driven touch input to e.g., a photodiode [56]. Similarly, it is possible to 3D print conductive material to directly integrate capacitive sensing electrodes into a model [44].

Although we did not initially set out to enable touch sensing for fabricated objects, the versatility of our technique naturally lends itself to this problem domain. Electrick can be easily applied to laser cut and 3D printed objects, as well as prototypes made from plastic, wood, ceramic, and other common non-conductive materials. As we will discuss, we can also directly 3D print and mold Electrick-capable objects using a low-cost conductive ABS.

SENSING PRINCIPLE

Electrick requires objects to have a conductive medium, either as its principle structural material, or as a surface coating. The object is further augmented with electrodes placed around the periphery of the desired interactive area. With this configuration, Electrick inserts a small AC current between a pair of adjacent electrodes (the *current-projecting* pair), creating an electric field in the conductive medium (Figure 1, left). The voltage difference is then measured at all other adjacent electrodes pairings (*voltage-*
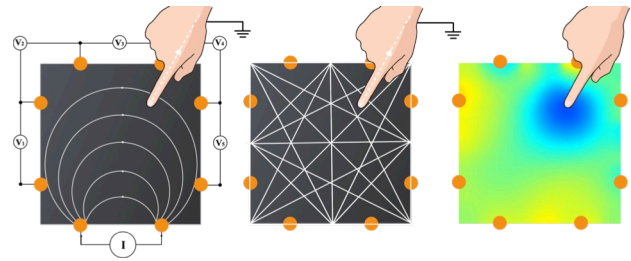

Figure 1. Left: we insert current from one pair of electrodes and measure voltage from other pairs. Center: A mesh of cross-sectional measurements. Right: A reconstructed 2D touch-sensing image. Blue indicates low current density.

measuring pairs). This process repeats for all combinations of *current-projecting* and *voltage-measuring* pairs, resulting in a mesh of cross-sectional measurements (Figure 1, center). This sensing scheme is similar to four-pole sensing in EIT systems (see e.g., [63] for more details).

As previously mentioned, our approach relies on the fact that a grounded object, such as a user's finger, will shunt some current to ground when it encounters an electric field through capacitive coupling (similar to surface capacitive screens [15] and in-air electric field sensing [61]). This current is very small, comparable to that induced by capacitive touch-screens found in smartphones. However, this shunting distorts the electric field, characteristically altering the voltages measured at receiver pairs. We can then use our cross-sectional measurements to recover the location of the shunt point (Figure 1, right).

Electrick can only be used with materials with compatible resistivity. If the resistivity is too high, the electric field will be very weak, making it hard to sense the field signal. However, if the surface resistivity is too low, the current shunted by the finger (a fairly high-impedance pathway) will be negligible, making touches hard to detect. In testing, we found that surface resistivity in the range of $500\,\Omega$ to 50 $M\Omega$ per square worked best for surface coat materials. The surface resistivity should be higher ($10\,k\Omega$ to $50\,M\Omega$) for structural materials, out of which objects can be directly 3D printed, milled or molded.

APPLICABLE MATERIALS & FABRICATION PROCESSES

We identified three classes of material of particular utility and interest: *solid*, *pliable*, and *paintable*. These basic material forms are used in a wide variety of fabrication and finishing processes, including subtractive methods (e.g., milling, laser cutting), additive methods (e.g., 3D printing), molding methods (e.g., stamping, casting, vacuum forming, blow molding, injection molding), and coating methods (e.g., brush painting, spray painting, powder coating).

Among many compatible materials, we sought low-cost examples with four key properties: 1) compatible electrical resistivity 2) non-toxicity 3) applied without exotic equipment or facilities, and 4) readily accessible. We now briefly discuss example materials we identified that fit our four criteria, and how they can be used with Electrick.
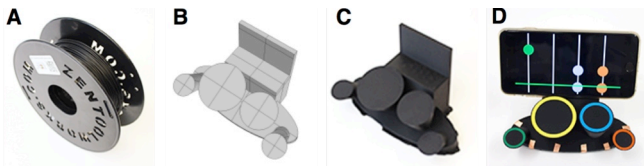
Figure 2. We used a carbon-loaded ABS filament (A) to 3D-print a custom phone accessory (B,C) for a phone game (D).

Example Solid Materials

Bulk plastics, such as ABS and Polycarbonate, are widely available in mildly conductive formulations (most often by adding carbon or metallic particles). These plastics come in many forms, including blocks (for e.g., milling), sheets (for e.g., forming/stamping), pellets (for e.g., molding/extrusion processes) and filament (for e.g., 3D printing).

As one example material, we use a static dissipating ABS, sold by Zen Toolworks as a filament (Figure 2A; $46 for a 1kg spool) [60]. At 45MΩ/sq, this black, carbon-loaded ABS is not sufficiently conductive for e.g., 3D printed circuits. However, it is perfect for 3D printing Electrick-capable objects (Figure 2C). We can also use the pellet form of this material to create molded objects (such as the mummy figurine seen in Figure 3A).

Another compatible material is Velostat, a carbon-loaded polyolefin sheet/film made by 3M [1]. It is primarily used for packaging of electronic components to mitigate electrostatic buildup. We ordered a 4mil thick, 3'×150' roll online for $200 (i.e., under 50 cents per square foot) [31], which has a surface resistivity of 72 kΩ/sq. This can be attached to surfaces directly (e.g., to walls), or laminated onto a thermal-formable sheet (e.g., polyethylene) and vacuum formed into a low-cost, durable shell of almost shape (Figure 4).

Example Pliable Materials

There are also conductive materials that are soft and pliable. As one example of an easy-to-use, off-the-shelf material, we selected Jell-O, which has a surface resistivity of roughly 12 kΩ/sq (Figure 22 offers an example application). Play-doh is also compatible with Electrick. We created our own using flour, water, salt, and food coloring to control the surface resistivity (roughly 23 kΩ/sq). Using Play-doh, users can shape objects with their bare hands and then make them interactive (example use shown in Figure 18).

Another pliable material is silicone, which is widely used in commercial molding/casting applications. We made our own conductive silicone by mixing bulk carbon fiber with standard silicone (1:18 ratio by weight). The outcome has a
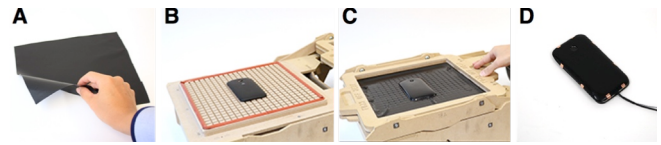
Figure 4. Velostat can be vacuum-formed, as seen in this phone enclosure example.

surface resistivity of ~16 MΩ/sq. From this material, we made a squishable, interactive Yoda toy (Figure 3B).

Example Paints

Liquid paint and spray coatings are particularly versatile, as they can be added as a postproduction step to almost *any* object or surface – small or large, flat or irregular, regardless of how the underlying object was manufactured. In addition to total paint coverage, paints can also be masked (e.g., stenciled, silk-screened) to define interactive areas.

As an example paint, we use a carbon conductive paint made by MG Chemicals [29], which is intended for electrostatic discharge and RF shielding uses. This paint can be purchased online as a 340g aerosol can for $16 [3] (Figure 5A), or as a liquid paint in quarts or gallons [32]. A single coat has resistivity of roughly 1kΩ/sq, and dries to a durable, matte black finish (Figure 5C).

Coatings

As previously discussed, the shunting effect of a user's finger occurs through capacitive coupling; direct contact is not required. This permits the use of an optional (thin) topcoat, which can be used to add color or alternate finish to an object. Although our search for compatible coatings was not exhaustive, we did experiment with spray (Figures 14 and 23), acrylic (Figure 5D), and latex paints (Figure 17), as well as paper (Figure 14).

IMPLEMENTATION

Our Electrick implementation required the development of custom hardware and software, which we now describe.

Electrodes

Once an object has been created or coated with a compatible conductive material, it must then be instrumented with electrodes around the periphery of the intended interactive region. In line with Electrick's low-cost DIY spirit, we used copper tape, to which we solder a wire that runs to our sensing board. It is also possible to reverse these fabrication steps, attaching the electrodes first, and then covering the electrodes with e.g., over-molded materials or paint.
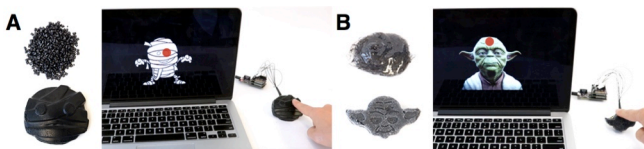

Figure 3. Conductive ABS (A) and silicone (B) can be cast, as seen in these toy examples. Touching different areas of these toys triggers different sounds and effects.

Figure 5. We carbon sprayed (A) an off-the-shelf toy (B) to make it interactive. A new topcoat was applied (C to D).
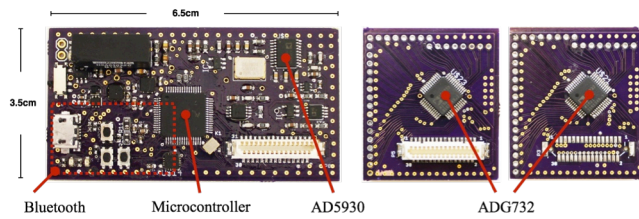
Figure 6. Left: Sensor motherboard. Right: two daughter boards with multiplexing functionality.

Sensing Board
Our custom sensing board is built around a Cortex M4 microcontroller running at 96 MHz (MK20DX256VLH7 [16]), powered by the Teensy 3.2 firmware [36] (Figure 6). The board has a voltage controlled current source (VCCS), direct digital synthesis (DDS) IC, and ADC preamp. The board also features multiplexers that allow for the cross-sectional measurements as well as a Bluetooth module to transmit data for wireless applications. The total cost of our hardware is $70, which could be made both smaller and less expensive in a high volume commercial application. A schematic view of our system is shown in Figure 7. Our current sensing board draws 120 mA during normal operation (including Bluetooth communication).

Excitation Signal
We use an AD5930 [5] DDS and an AD8220-based Voltage-controlled current source (VCCS) [6] to generate an electric field. The DDS is configured to output 200 kHz sinusoidal waves. The signal is then fed into the VCCS to output a constant AC current. Our sensor can drive up to 6 Vpp to maintain a constant AC current excitation. To improve SNR, we increased the current for low-resistance materials, and decreased it for high-resistance ones. As a result, input current levels varied across test cases (maximally 0.42 mA in the lowest-resistance, carbon-sprayed panel).

Multiplexing
A pair of 32-to-1 multiplexers [4] connect the VCCS terminals to two electrodes, forming the *current-projecting* electrode pair. Another pair of multiplexers connects two other electrodes (the *voltage-measuring* pair) to the preamp buffer terminals. This electrode selection flexibility also affords us the flexibility to vary the number of electrodes used (i.e., 8, 16, or 32).

Analog Sampling
The measured signal is amplified with a preamp to maximize the dynamic range of our ADC. We also implemented a
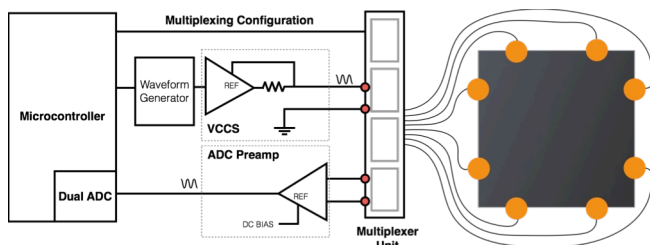
79.6 kHz high pass filter to dampen ambient EM noise, chiefly fluorescent light ballasts (i.e. 50 kHz) and power-line noise (i.e. 60 Hz). The input signal is then biased by AVDD/2 (1.65 V) and sampled by our microcontroller's ADCs at 4 MHz with 12-bit resolution. We used our microcontroller's two ADCs in an interleaved DMA mode to achieve this high sampling rate.

Data Acquisition
After our board selects the appropriate electrodes using its multiplexers, it waits 100 μs for the DC bias on the AC coupling capacitors to stabilize. The board then collects 200 samples (roughly 10 periods of our 200 kHz excitation signal) for a root-mean-square (RMS) computation. This constitutes a single measurement (taking ~137 μs in total).

The board then moves to the next voltage-measuring electrode pair, reconfiguring its multiplexers accordingly. After collecting all measurements for the current-projecting configuration, the board then moves to the next current-projecting pair and repeats the above procedure. Once it completes one full frame of measurements (all current-projecting pairs), the board sends the values over Bluetooth or USB to a laptop for further processing. Table 1 provides the number of measurements required when using different electrode counts, which also defines the system frame rate (as each measurement takes ~137 μs).

Number of Electrodes	8	16	32
Number of Measurements req. per Frame	40	208	928
Sensing Frame Rate (Hz)	181	35	8

Table 1. The number of measurements required per frame and the resulting sensing FPS for different electrode counts.

Touch Tracking
We initially developed our finger-tracking pipeline using a fully realized tomographic reconstruction, to which we applied standard computer vision "blob" tracking techniques (Figure 8). Specifically, we used a single step Gauss-Newton method using a maximum a posteriori estimator [7] to produce our tomographic reconstruction (provided by the EIDORS EIT toolkit [53]). On a MacBook Pro with a 2.7 GHz Intel Core i5 processor, the solver takes 1.98, 2.56 and 3.01 ms for 8, 16 and 32 electrode inputs respectively.

This approach is capable of high accuracy and even multi-touch segmentation (Figure 8, right). However, it requires construction of a finite element model (FEM) for each object before use [25]. This is relatively straightforward for planar circular or rectilinear surfaces, but is a significant obstacle for ad hoc uses and complex geometries (which would require 3D scanning equipment). We also found this method to be sensitive to small fabrication/manufacturing variances, such as electrode size, adhesion, and conductive coating thickness.

Fortunately, machine learning offers a robust and practical alternative, one that offloads much of this variability and complexity from users to computers. Instead of having to

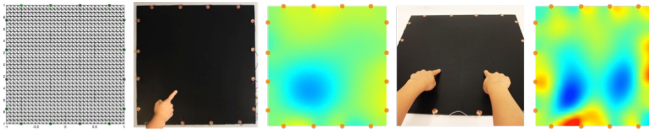**Figure 7. A schematic view of our system with e.g., 8 electrodes.**

Figure 8. From left to right: Finite Element Model, 60×60 cm touch panel, reconstructed touch image, two fingers touching, and reconstructed touch image.

model an object's geometry, users can perform a simple one-time calibration on the object itself, from which machine learning models can be initialized. In addition to permitting arbitrary geometries, this process also innately captures and accounts for variances in fabrication. For input features, we simply use our raw cross-sectional measurements with no additional featurization. Thus the lengths of the feature sets can be found in Table 1 ("Number of Measurements required per Frame" row).

Two classification approaches are possible. For sensing *discrete* touch positions (e.g., buttons), we used a classification model (built using Weka [23], SMO, RBF kernel with γ=0.07). The same parameters are used for models that distinguish between touch and no-touch states. To support *continuous* 2D touch tracking, we used two independent regression models (SMOReg, RBF kernel with γ=0.01) operating in parallel – one for X and another for Y position.

Multitouch
Tomographic techniques output a 2D reconstruction of the sensed medium. As such, localizing multiple finger touches is immediately possible, as can be seen in Figure 8 (right). Standard computer vision techniques, most notably blob detection, can be applied. However, due to the low resolution of the reconstruction, there must be substantial separation between finger contacts for robust tracking. Anecdotally, with Electrick, this has to be at least 10 cm, irrespective of material and electrode configuration. Our preliminary investigations are promising, but we leave a full exploration of multitouch capabilities for future work.

EVALUATION
The versatility of Electrick meant there was a range of factors we wished to investigate: the performance across different electrode counts (*8, 16, 32*), materials (*Velostat, carbon spray, carbon ABS*), surface sizes (*15×15, 30×30, 60×60 cm*), surface geometries (*flat, curved, angular*), and coatings (*bare, paper, spray paint*). Within each evaluation, we tested the performance of our discrete touch sensing and continuous tracking approaches. It was not feasible to run a full 3×3×3×3×3 factors design, so we instead structured our evaluation as a series of focused experiments, taking a total of 70 minutes to complete. We recruited 14 participants (8 female, mean age 26), who were compensated $20.

Apparatus
To best capture our system's performance and not user inaccuracies, we employed a template to guide user touches. This was a 15×15 cm laser-cut sheet of (non-conductive) acrylic with a 4×4 grid of 1.5 cm holes (Figure 9, left). This
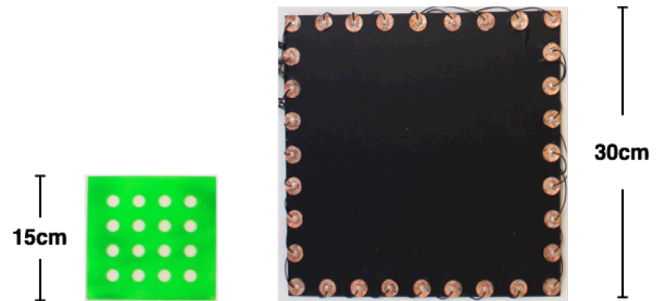

Figure 9. Evaluation template next to 30×30 cm panel with 32 electrodes.

was overlaid onto the experimental surface. Our test apparatus varied slightly across our five experiments. For factors within our control, we selected values with intermediate performances, for example, all of our experiments used 16-electrode sensing (except, of course, for the electrode count experiment). We now describe the particular conditions and apparatus of our five experiments:

Electrode Count – To ensure adequate space for electrodes, we used a 30×30 cm Velostat sheet augmented with 32 electrodes (Figure 9, right). Our board configured itself for 8, 16 or 32 electrode modes in software.

Material – We selected three very different materials: Velostat, conductive ABS, and carbon paint. Due to the limited bed size on our 3D printer, we made all three of our material conditions 15×15 cm in size. Carbon Spray and Velostat were applied to 1/8" thick acrylic sheets, while the ABS condition was printed monolithically with 1 mm thickness (Figure 11).

Surface Size – We tested three surface sizes: 15×15, 30×30 and 60×60 cm (Figure 12). These were all flat, Velostat-laminated acrylic sheets. We randomized the touch template location on the 30×30 and 60×60 cm touch panels per user.

Surface Geometry – In order to test surface geometry in a controlled way, we 3D printed (using conventional filament) three 15×15 cm panels with varying surface features: flat, curved and angular (Figure 13). The latter two 3D conditions had a Z-variance of 1 cm, making them more "2.5D". However, as we will show in our Example Applications, more extreme 3D geometries are possible. To conform to the irregular surface, we used carbon spray as our conductive material. The irregular geometry also prevented us from using our flat acrylic touch template, and so touch points were denoted by painted white circles.

Coating – We tested three coating conditions: bare (i.e., unmodified), paper-coated, and spray-painted (conventional white paint). These coatings were applied to a flat, carbon-sprayed, acrylic sheet 15×15 cm in size (Figure 14).

Procedure
We employed the same procedure for all five experiments, the order of which was randomized. When first presented with a surface condition, we asked participants to hold their

finger roughly 5 cm away from the surface. Over a period of roughly one second, 30 data points were recorded and labeled as "no touch". Participants were then instructed to touch each of the 16 points denoted by the touch template. This was done one at a time, in a random order, as requested by a simple visualization on a laptop screen. Each time a user touched a point, 30 data points were recorded. The laptop emitted a beep when the user could proceed to the next point. This concluded one round of data collection, the *only* training data we collected.

This data was then used to train our touch-sensing machine learning models. For discrete touch location sensing, data was used to train a touch/no-touch classifier and an independent, 16-class classifier – one class for each touch location. For our regression-based, continuous touch-tracking model, only data from the four corners was used for training. This mitigates overfitting and offers a more realistic evaluation of accuracies (vs. training on all 16 points).

We then tested our system's accuracy *live* (i.e., no post hoc calibration, algorithm tweaks, data cleaning, etc.). We followed the same procedure as above, where users moved sequentially through all touch points in a random order. This time, the system's live classification/regression result was recorded along with the requested touch location for later analysis. This testing procedure was repeated twice more, for three testing rounds in total. This four-round procedure (1 training round followed by 3 testing rounds) was repeated for every condition in all five experiments.

RESULTS

We now discuss the results of our five experiments, as well as a post hoc study investigating sensing stability across users. All figures use standard error for their error bars.

Touch Segmentation

Touch/no-touch classification accuracy averaged 99.5% (SD=0.5) across all conditions and factors. The one significant outlier ($p<0.05$) from this average was our paper-coated condition (93.2% accuracy).

Number of Electrodes

The touch tracking accuracy across our three electrode count conditions is shown in Figure 10. Our discrete touch location classifier achieved 90.7% (SD=12.0%) mean accuracy. Of note, 57.0% of the error trials were in adjacent positions (i.e., off by one cell in our 4×4 touch grid). Our regression-based, continuous tracking method had a mean distance error of 9.1 mm (SD=4.7).

Intuitively, we expected higher electrode counts to produce a finer mesh of cross-sectional measurements, and thus offer more accurate touch tracking. However, we found the opposite effect: a paired t-test showed that the 32-electrode condition was significantly worse than the 8-electrode condition ($p<0.05$) in the case of discrete tracking. As an additional visualization, we also plot touch trials from all participants (raw; no post hoc per-user offsets, etc.) along with 2σ ellipses drawn to scale (Figure 10).

We suspect this reduction in accuracy is chiefly due to the reduced distance between projecting/measuring electrode pairs. A shorter electrode separation means that the electric field does not project as far into the conductive medium, which reduces the signal-to-noise ratio (SNR). Furthermore, the reduced distance between measuring electrode pairs similarly decreases terminal resistance, resulting in smaller voltage measurements, again reducing SNR. This result suggests that electrode count should be tuned according to surface size; e.g., for smaller interactive areas, lower electrode counts are likely to work better.

Material

Our material experiment results, seen in Figure 11, show an average discrete touch accuracy of 91.4% (SD=9.6), with
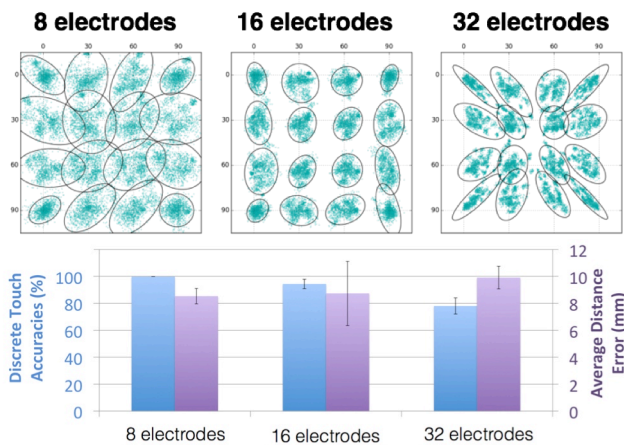

Figure 10. Evaluation results for electrode count experiment. Top: touch point distributions with 2σ ellipses. Bottom: Discrete touch and continuous tracking accuracies.
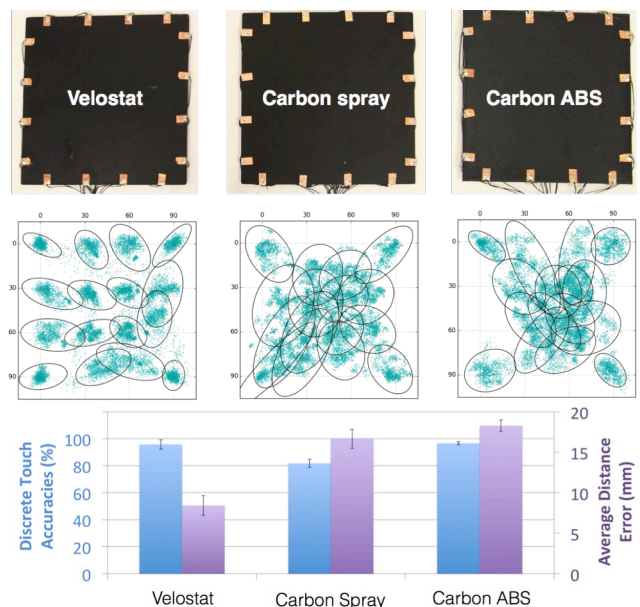

Figure 11. Evaluation results for material experiment. Top: 15×15 cm touch panels coated using the three materials. Middle: touch point distributions with 2σ ellipses. Bottom: Discrete touch and continuous tracking accuracies.
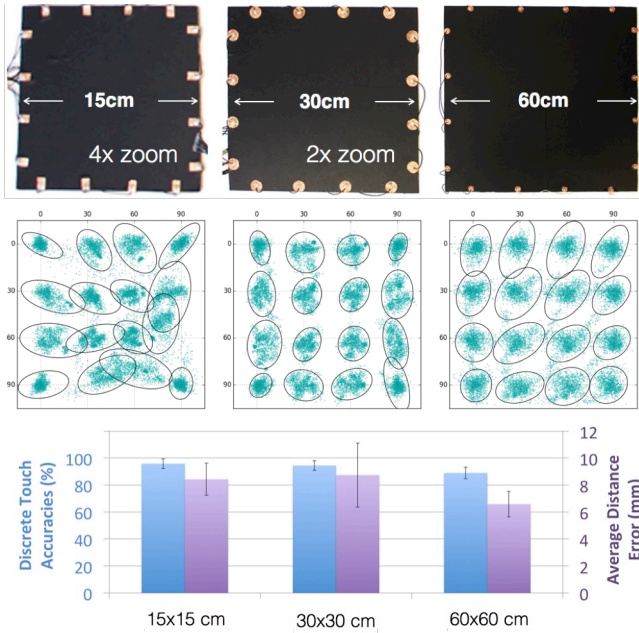
Figure 12. Evaluation results for surface size experiment. Top: touch panels of different sizes. Middle: touch point distributions with 2σ ellipses. Bottom: Discrete touch and continuous tracking accuracies.

84.8% of errors in adjacent positions. Continuous touch tracking had a mean distance error of 14.4 mm (SD=3.8); a paired t-test shows a significant difference between Velostat and our other two test materials (p<0.05). We suspect this is a result of Velostat's superior homogeneity (compared to our other two conditions), as it is an industrially manufactured material. This makes the electric field projection more linear, whereas small non-linearities in our Carbon Spray and Carbon ABS conditions meant our tracking regressions could not accurately interpolate interior touches. A more controlled coating process would likely yield improve accuracy. In addition, note in Figure 11 that positional accuracy improves towards the corners. This suggests that a denser calibration pattern (as opposed to a sparse, four-corner one) could compensate for such material variances.
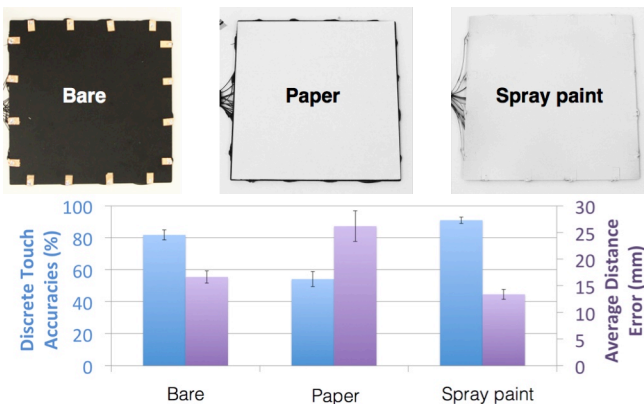

Figure 14. Evaluation results for coating experiment. Top: touch panels of different coating materials. Bottom: Discrete touch and continuous tracking accuracies.
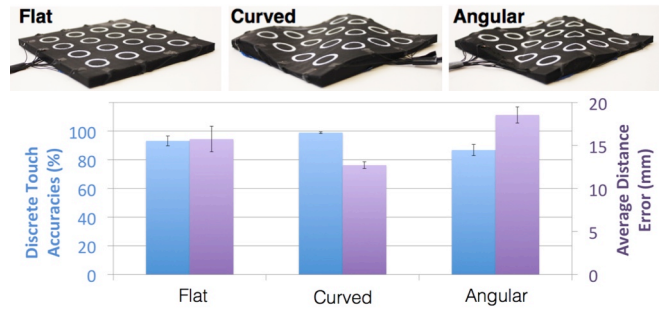

Figure 13. Evaluation results for geometry experiment. Top: touch panels of different geometries. Bottom: Discrete touch and continuous tracking accuracies.

Surface Size

Figure 12 shows the results of our surface size experiment. The average classification accuracy for discrete touch locations was 93.0% (SD=14.3), with 95.7% of errors in adjacent locations. Mean continuous finger tracking distance error was 7.9 mm (SD=5.6). Interestingly, we found that larger surfaces tend to have more linear regression results, though there was no significant difference between our three conditions. This is probably not directly related to size *per se*, but rather tied to our earlier observation about electrode separation (i.e., as surface size increases, so does electrodes electrode separation, improving accuracy).

Surface Geometry

There was no statistically significant differences between our three surface geometries (Figure 13). The average discrete touch accuracy was 92.9% (SD=9.8), with 80.3% of the errors in adjacent locations. Meanwhile, continuous touch tracking mean distance error was 15.7 mm (SD=3.5).

Coatings

Figure 14 shows the results from our coating experiment. Encouragingly, s*pray paint* and *bare* performed equally well, suggesting some coatings are immediately compatible with Electrick, opening a range of finish and color options. However, the *paper* covering resulted in significantly worse performance (p<0.05) than both other methods, likely because paper is thicker than a spray coat, and thus impacts capacitive coupling more substantially.

Stability Across Users

We employed a train-test experimental procedure in our main evaluation in order to test our system *live*, which offers an honest appraisal of real world accuracies. However, we recorded all data, including raw sensor values, permitting us to run a post hoc study utilizing all collected data.
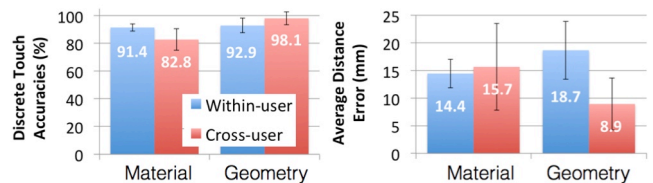

Figure 15. Within-user accuracies and cross-user accuracies for the material and geometry experiments.

Figure 16. Stickers can be placed (A) and bound (B) to laptop functions (C), creating press-able shortcuts (D).

Figure 17. A user can turn on/off a light by tapping the wall. Brightness can be adjusted by sliding up and down.

In particular, we were curious if Electrick's sensing was *user-dependent*, or if the touch sensing was *universal* across users. To explore this, we ran a leave-one-user-out crossfold validation experiment. In each fold, Electrick was allowed to train on 13 users' data, and then tested on a data from a 14th user. We repeated this process for all user combinations. This effectively simulates "walk up" accuracy, wherein the system has never previously seen the user.

We ran this post hoc test using data from our material and geometry studies, the results of which are shown in Figure 15. Overall, discrete touch location classification accuracy decreases by a mean of 3.3%, while continuous touch tracking improves by 2.5 mm. These modest fluctuations, neither of which is statistically significant, suggest that Electrick can be trained (e.g., factory calibrated) on a small subset of users and then work for all.

EXAMPLE APPLICATIONS

To demonstrate the expressivity and versatility of Electrick, we built a variety of fully functional, interactive, example applications. These were selected to include a range of sizes, geometries, materials, fabrication processes and use domains. They are best understood by viewing our Video Figure, but we include brief descriptions below.

Desk: Using a roller, we carbon painted a desk and attached eight electrodes to the sides of the desktop, allowing the whole surface to become touch sensitive. As an example application, users can place paper stickers anywhere on the table, register them to an application (e.g., browser) or function (e.g., mute), after which the stickers can be pressed to quick launch items (Figure 16).

Figure 20. This Electrick-augmented steering wheel can track hand location and gestures.

Figure 18. A Play-doh snowman is made interactive.

Figure 19. A guitar with dynamically configurable controls.

Wall: We also carbon painted a 4x8' sheet of drywall (Figure 17). By using 16 electrodes, we created a 107" diagonal touch surface. We then applied an off-white latex wall paint. Pervasive touch-sensitive walls could enable innumerable applications. As one example, we created a light control application; tapping the wall anywhere near a sconce light toggles it on/off; dragging up or down allows the user to control the brightness.

Toys: The low-cost nature of toys has largely precluded the integration of touch surfaces. As an example of how Electrick can be used in this domain, we carbon sprayed a dog toy and then hand painted it in colored acrylic paints (Figure 5). With this setup, touches to different locations trigger different audio effects. We made similar apps for toys molded from conductive ABS and silicone (Figure 3).

Play-doh: Play-doh can also be made interactive with Electrick, allowing a user to sculpt a figure or object, and then bind interactive functionally to different touch locations. To achieve this, the finished object is placed onto an 8-electrode base, with small pins that penetrate the play-doh. Figure 18 offers a snowman example, where different phrases are spoken when touching the nose or belly.

Guitar: In this demo, a user can add virtual controls (e.g. volume, filters and effects) to the surface of a guitar through a drag-and-drop design application on a computer (Figure 19). To achieve touch tracking, we carbon sprayed an electric guitar and used eight electrodes running along the edge of the instrument.

Car Steering Wheel: This is a perfect example of a large, irregular object that has yet to be instrumented with rich touch functionality, despite offering an immediately useful surface for user input. As an example, we added 8 electrodes to a carbon-sprayed Chevy Aveo steering wheel; Electrick can track the position of both hands, as well as detect gestures, such as swipes (Figure 20).

Phone Case: We vacuum-formed a rear cover for a Moto E smartphone (Figure 4). With Electrick, phone enclosures

Figure 21. This Electrick-augmented phone enclosure allows different grips to launch apps.
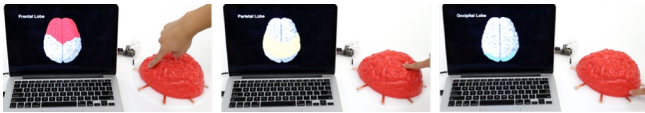
Figure 22. Students can touch different parts of this Jell-O cast to learn about the different regions of the human brain.
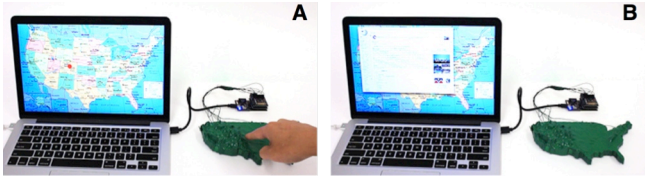

Figure 23. In this interactive topographical map, touching different regions launches local information.

could not only provide protection, but also be used to detect various grips, to e.g., quickly launch apps, such as the camera or messaging (Figure 21)

Instructional Aids: Physical props are often useful in learning visual-spatial subject matter. As an example, we cast a model of a brain using Jell-O, simulating the organic feel. By placing the model onto an 8-electrode acrylic base, students can touch different regions of the brain to summon information (Figure 22). Such a base could be reused for any number of low-cost instructional objects. Similarly, we coated a US topographical map with carbon spray, instrumented it with eight electrodes, and applied a green topcoat with spray paint (Figure 23). Information about different geographical regions is retrieved upon a user's touch.

Bongo Hero: We designed a "pluggable" phone accessory featuring four miniature bongos (Figure 2). This was 3D printed using carbon ABS on an off-the-shelf MakerBot Replicator 2X (standard ABS settings, 10% infill). To this, we attached eight electrodes around the base, allowing this otherwise static 3D print to become touch interactive. In this example, we enable a "bongo hero" game (Figure 2D).

Game Controller: Finally, we laser cut a basic game controller, to which we added a Velostat layer and eight electrodes (Figure 24, left). With the surface now made touch sensitive, players or developers can pick (or customize) different interface layouts by overlaying different templates (Figure 24, bottom row). Not only are buttons supported, but also analog inputs, like sliders and joysticks. Obviously, this design flexibility has immediate implications and applications in rapid prototyping of physical interfaces.
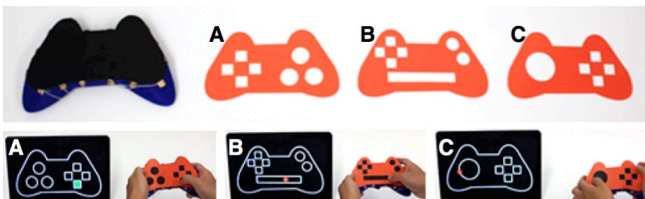

Figure 24. This Electrick-powered game controller allows different layouts to be easy swapped in.

DISCUSSION

One potential concern with Electrick is durability, especially of coatings. We did not detect wear in any of the objects we created (all pictures in the evaluation section were taken after the user study, during which each touch surface was touched 896 times by participants). Of course, this is not a long duration and there was no exposure to the elements. Also, no doubt, there are many more materials that are compatible with Electrick – such as conductive rubbers, foams and fabrics – which we did not have a chance to explore. Transparent coatings may even be possible (e.g., ITO or PEDOT). And of course, conductive material composites can often be made in the home or lab by mixing conventional and conductive materials (e.g., carbon powder), as we did with silicone.

We did find that environmental electromagnetic noise, from e.g., fluorescent lights, running appliances and power lines, can affect tracking accuracy. Not only does the conductive object act like an antenna, but so does the human body, which upon touch, introduces more noise. As discussed previously, we used a high pass filter to combat this interference, though we still found being proximate to (e.g., standing underneath) a florescent light reduced performance. We hope to explore ways to mitigate this in future work.

Finally, perhaps the biggest limitation stems from the grounding condition, which is a universal issue for Electric Field Sensing systems [19]. In Electrick, both the sensor and the user's body capacitively couples to common ground (the Earth) to complete the circuit. Bigger sensor ground planes have stronger capacitive coupling, and thus bigger shunting current and SNR. In our user study, the sensor was connected to and powered by a laptop (under both plugged-in and unplugged conditions; no statistically significant difference in performance), which offered a fairly substantial ground. When a smaller sensor ground is used (e.g., running from a small LiPo battery), the shunting current will be reduced. Although our sensor has a high input impedance, this decrease in shunting current will inevitably lower the SNR. This may preclude the ability to use Electrick in small form factors, such as wearables, though we do believe Electrick can be made to work in devices as small as smartphones.

CONCLUSION

We have presented Electrick, a low-cost and versatile touch sensing technique that can be scaled to large surfaces and irregular geometries. We further show that our technique can be used to bring touch interactivity to rapidly prototyped objects, including those that are 3D printed. Through a series of user studies, we characterized the performance characteristics of our system. Our results show that Electrick can accurately track both discrete and continuous touch input under various test conditions, materials, shapes and sizes. It is also is robust over time and across users. We believe this work can bring touch interactivity to new classes of objects, as well as enable designers to rapidly prototype objects with innate interactive capabilities.

REFERENCES
1. 3M Material Safety Data Sheet. Retrieved January 5, 2017 from http://multimedia.3m.com/mws/mediawebserver?66666 UtN&ZUxL99XlX&ynxM_4Vu9KcuZgVU_LXT1u66 6666--

2. 3M Multi-Touch Display C5567PW. Datasheet. Retrieved December 26, 2016 from http://multimedia.3m.com/mws/media/1082683O/3m-multi-touch-display-c5567pw.pdf

3. Amazon Product Details. Retrieved January 5, 2017 from https://amzn.com/B008OA931A

4. Analog Devices. 32-Channel Analog Multiplexer. ADG732. Retrieved January 5, 2017 from http://www.analog.com/media/en/technical-documentation/data-sheets/ADG726_732.pdf

5. Analog Devices. Programmable Frequency Sweep and Output Burst Waveform Generator. AD5930. Retrieved January 5, 2017 from http://www.analog.com/media/en/technical-documentation/data-sheets/AD5930.pdf

6. Analog Devices. JFET Input Instrumentation Amplifier with Rail-to-Rail Output in MSOP Package. Retrieved January 5, 2017 from http://www.analog.com/media/en/technical-documentation/data-sheets/AD8220.pdf

7. Andy Adler and Robert Guardo. 1996. Electrical impedance tomography: regularized imaging and contrast detection. IEEE transactions on medical imaging 15, 2. 170–179. http://doi.org/10.1109/42.491418

8. Eric Akaoka, Tim Ginn, and Roel Vertegaal. 2010. DisplayObjects: prototyping functional physical interfaces on 3d styrofoam, paper or cardboard models. In Proceedings of the fourth international conference on Tangible, embedded, and embodied interaction (TEI '10). ACM, New York, NY, USA, 49-56. http://doi.org/10.1145/1709886.1709897

9. Hassan Alirezaei, Akihiko Nagakubo, and Yashuo Kuniyoshi. 2009. A tactile distribution sensor which enables stable measurement under high and dynamic stretch. In Proceedings of the IEEE Symposium 3D User Interfaces. 87–93. http://doi.org/10.1109/3DUI.2009.4811210

10. Thomas Augsten, Konstantin Kaefer, René Meusel, Caroline Fetzer, Dorian Kanitz, Thomas Stoff, Torsten Becker, Christian Holz, and Patrick Baudisch. 2010. Multitoe: high-precision interaction with back-projected floors based on high-resolution multi-touch

11. D'Antona, G., Ferrero, A., Lazzaroni, M., Ottoboni, R. and Samarani, E. 2002. Active monitoring apparatus for underground pollutant detection based on electrical impedance tomography. In Proceedings of the IEEE Instrumentation and Measurement Technology Conference. 577–579. http://doi.org/10.1109/IMTC.2002.1006906

12. Beginner's Mind Collective and David Shaw. 2012. Makey Makey: improvising tangible and nature-based user interfaces. In Proceedings of the 6th International Conference on Tangible, Embedded and Embodied Interaction (TEI '12). ACM, New York, NY, USA, 367-370. http://doi.org/10.1145/2148131.2148219

13. Gabe Cohn, Sidhant Gupta, Tien-Jui Lee, Dan Morris, Joshua R. Smith, Matthew S. Reynolds, Desney S. Tan, and Shwetak N. Patel. 2012. An ultra-low-power human body motion sensor using static electric field sensing. In Proceedings of the 2012 ACM Conference on Ubiquitous Computing (UbiComp '12). ACM, New York, NY, USA, 99-102. http://doi.org/10.1145/2370216.2370233

14. Gabe Cohn, Daniel Morris, Shwetak N. Patel, and Desney S. Tan. 2011. Your noise is my command: sensing gestures using the body as an antenna. In Proceedings of the SIGCHI Conference on Human Factors in Computing Systems (CHI '11). ACM, New York, NY, USA, 791-800. http://doi.org/10.1145/1978942.1979058

15. Blair Evans. 1989. Method of and apparatus for sensing the location, such as coordinates, of designated points on an electrically sensitive touch-screen surface, Google Patents.

16. Freescale Microcontroller Datasheet. Retrieved January 5, 2017 from http://cache.freescale.com/files/32bit/doc/data_sheet/K 20P64M72SF1.pdf

17. Jerry Alan Fails and Dan Olsen Jr. 2002. Light widgets: interacting in every-day spaces. In Proceedings of the 7th international conference on Intelligent user interfaces (IUI '02). ACM, New York, NY, USA, 63-69. http://doi.org/10.1145/502716.502729

18. Mathieu Le Goc, Stuart Taylor, Shahram Izadi, and Cem Keskin. 2014. A low-cost transparent electric field sensor for 3d interaction on mobile devices. In Proceedings of the SIGCHI Conference on Human Factors in Computing Systems (CHI '14). ACM, New York, NY, USA, 3167-3170. http://doi.org/10.1145/2556288.2557331

19. Tobias Grosse-Puppendahl, Christian Holz, Gabe Cohn, Raphael Wimmer, Oskar Bechtold, Steve Hodges, Matthew Reynolds, and Joshua R. Smith. 2017.

Finding Common Ground: A Survey of Capacitive Sensing in Human-Computer Interaction. In Proceedings of the 35th Annual ACM Conference on Human Factors in Computing Systems (CHI '17). ACM, New York, NY, USA. http://doi.org/10.1145/3025453.3025808

20. Chris Harrison and Scott E. Hudson. 2008. Scratch input: creating large, inexpensive, unpowered and mobile finger input surfaces. In Proceedings of the 21st annual ACM symposium on User interface software and technology (UIST '08). ACM, New York, NY, USA, 205-208. http://doi.org/10.1145/1449715.1449747

21. David Holman and Roel Vertegaal. 2011. TactileTape: low-cost touch sensing on curved surfaces. In Proceedings of the 24th annual ACM symposium adjunct on User interface software and technology (UIST '11 Adjunct). ACM, New York, NY, USA, 17-18. http://doi.org/10.1145/2046396.2046406

22. Eun-Soo Hwang, Jung-hoon Seo, and Yong-Jun Kim. 2007. A Polymer-Based Flexible Tactile Sensor for Both Normal and Shear Load Detections and Its Application for Robotics. Journal of Micromechanical Systems Vol. 16, No. 3, 556-563. http://doi.org/10.1109/JMEMS.2007.896716

23. Mark Hall, Eibe Frank, Geoffrey Holmes, Bernhard Pfahringer, Peter Reutemann, and Ian H. Witten. 2009. The WEKA data mining software: an update. SIGKDD Explor. Newsl. 11, 1. 10-18. http://doi.org/10.1145/1656274.1656278

24. Scott E. Hudson and Jennifer Mankoff. 2006. Rapid construction of functioning physical interfaces from cardboard, thumbtacks, tin foil and masking tape. In Proceedings of the 19th annual ACM symposium on User interface software and technology (UIST '06). ACM, New York, NY, USA, 289-298. http://doi.org/10.1145/1166253.1166299

25. Hemant Jain, David Isaacson, Peter M Edic, and Jonathan C Newell. 1997. Electrical Impedance Tomography of Complex Conductivity Distributions with Noncircular Boundary. 44, 11: 1051–1060. http://doi.org/10.1109/10.641332

26. Philip T. Krein and R. David Meadows. 1990. The electroquasistatics of the capacitive touch panel. IEEE Transactions on Industry Applications Volume: 26, Issue: 3, 529 – 534. http://doi.org/10.1109/28.55954

27. LG Inc. Media cover. Retrieved January 5, 2017 from http://www.theverge.com/2016/1/3/10706180/lg-rollable-display-flexible-screen-announced-ces-2016

28. Gierad Laput, Eric Brockmeyer, Scott E. Hudson, and Chris Harrison. 2015. Acoustruments: Passive, Acoustically-Driven, Interactive Controls for Handheld Devices. In Proceedings of the 33rd Annual ACM Conference on Human Factors in Computing Systems (CHI

'15). ACM, New York, NY, USA, 2161-2170. http://doi.org/10.1145/2702123.2702414

29. MG Chemicals Inc: http://www.mgchemicals.com

30. Microsoft Surface Hub. User Guide. Retrieved January 5, 2017 from https://microsoft.com/microsoft-surface-hub/en-us

31. Mouser product page. Retrieved January 5, 2017 from http://www.mouser.com/ProductDetail/SCS/1704-36

32. MTE Solutions Product Details. Retrieved January 5, 2017 from http://shop.mtesolutionsinc.com/new-from-mg-chemicals/mg-chemicals-838ar-3-78l-carbon-conductive-coating/

33. Adiyan Mujibiya and Jun Rekimoto. 2013. Mirage: exploring interaction modalities using off-body static electric field sensing. In Proceedings of the 26th annual ACM symposium on User interface software and technology (UIST '13). ACM, New York, NY, USA, 211-220. http://doi.org/10.1145/2501988.2502031

34. Maggie Orth, Rehmi Post, and Emily Cooper. 1998. Fabric computing interfaces. In Proceedings of the SIGCHI Conference on Human Factors in Computing Systems (CHI '98). ACM, New York, NY, USA, 331-332. http://doi.org/10.1145/286498.286800

35. Makoto Ono, Buntarou Shizuki, and Jiro Tanaka. 2013. Touch & activate: adding interactivity to existing objects using active acoustic sensing. In Proceedings of the 26th annual ACM symposium on User interface software and technology (UIST '13). ACM, New York, NY, USA, 31-40. http://doi.org/10.1145/2501988.2501989

36. PJRC Inc Product Detail. Retrieved January 5, 2017 from https://www.pjrc.com/teensy/teensy31.html

37. Pham, D.T., Ji, Z., Peyroutet, O., Yang, M., Wang, Z. and Al-Kutubi, M. 2006. Localization of impacts on solid objects using the wavelet transform and maximum likelihood estimation. In Proceedings of IPROMS '06. 541–547. http://doi.org/10.1016/B978-008045157-2/50095-X

38. Ganna Pugach, Alexandre Pitti, and Philippe Gaussier. 2015. Neural learning of the topographic tactile sensory information of an artificial skin through a self-organizing map. Advanced Robotics, Volume 29 Issue 21: Robotic Sensor Skins. 1393-1409. http://doi.org/10.1371/journal.pone.0026561

39. Ivan Poupyrev, Chris Harrison, and Munehiko Sato. 2012. Touché: touch and gesture sensing for the real world. In Proceedings of the 2012 ACM Conference on Ubiquitous Computing (UbiComp '12). ACM, New York, NY, USA, 536-536. http://doi.org/10.1145/2370216.2370296

40. Ivan Poupyrev, Nan-Wei Gong, Shiho Fukuhara, Mustafa Emre Karagozler, Carsten Schwesig, and Karen E. Robinson. 2016. Project Jacquard: Interactive Digital

Textiles at Scale. In Proceedings of the 2016 CHI Conference on Human Factors in Computing Systems (CHI '16). ACM, New York, NY, USA, 4216-4227. http://doi.org/10.1145/2858036.2858176

41. Joseph A. Paradiso, Che King Leo, Nisha Checka, and Kaijen Hsiao. 2002. Passive acoustic knock tracking for interactive windows. In CHI '02 Extended Abstracts on Human Factors in Computing Systems (CHI EA '02). ACM, New York, NY, USA, 732-733. http://doi.org/10.1145/506443.506570

42. Joshua R. Smith. 1995. Toward Electric Field Tomography. M.S. Thesis. Massachusetts Institute of Technology, Cambridge, MA.

43. Joshua R. Smith. 1999. Electric field imaging. Ph.D. Dissertation. Massachusetts Institute of Technology, Cambridge, MA.

44. Martin Schmitz, Mohammadreza Khalilbeigi, Matthias Balwierz, Roman Lissermann, Max Mühlhäuser, and Jürgen Steimle. 2015. Capricate: A Fabrication Pipeline to Design and 3D Print Capacitive Touch Sensors for Interactive Objects. In Proceedings of the 28th Annual ACM Symposium on User Interface Software & Technology (UIST '15). ACM, New York, NY, USA, 253-258. http://doi.org/10.1145/2807442.2807503

45. Valkyrie Savage, Andrew Head, Björn Hartmann, Dan B. Goldman, Gautham Mysore, and Wilmot Li. 2015. Lamello: Passive Acoustic Sensing for Tangible Input Components. In Proceedings of the 33rd Annual ACM Conference on Human Factors in Computing Systems (CHI '15). ACM, New York, NY, USA, 1277-1280. http://doi.org/10.1145/2702123.2702207

46. Valkyrie Savage, Colin Chang, and Björn Hartmann. 2013. Sauron: embedded single-camera sensing of printed physical user interfaces. In Proceedings of the 26th annual ACM symposium on User interface software and technology (UIST '13). ACM, New York, NY, USA, 447-456. http://doi.org/10.1145/2501988.2501992

47. Valkyrie Savage, Sean Follmer, Jingyi Li, and Björn Hartmann. 2015. Makers' Marks: Physical Markup for Designing and Fabricating Functional Objects. In Proceedings of the 28th Annual ACM Symposium on User Interface Software & Technology (UIST '15). ACM, New York, NY, USA, 103-108. http://doi.org/10.1145/2807442.2807508

48. Valkyrie Savage, Xiaohan Zhang, and Björn Hartmann. 2012. Midas: fabricating custom capacitive touch sensors to prototype interactive objects. In Proceedings of the 25th annual ACM symposium on User interface software and technology (UIST '12). ACM, New York, NY, USA, 579-588. http://doi.org/10.1145/2380116.2380189

49. Eckhard Teschner, Michael Imhoff, and Steffen Leonhardt. 2015. Electrical Impedance Tomography: The realization of regional ventilation monitoring, 2nd Edition. Dräger Medical GmbH, Germany.

50. Treetronic. 2015. PiCUS: Treetronic, Electric Resistance Tomography. Retrieved January 5, 2017 from http://www.argus-electronic.de/en/content/download/431/4060/.../ TreeTronic+3+manual.pdf

51. David Silvera Tawil, David Rye, and Mari Velonaki. 2011. Touch Modality Interpretation for an EIT-Based Sensitive Skin. In Proceedings of the IEEE Conference on Robotics and Automation (ICRA). 3770–3776. http://doi.org/10.1109/ICRA.2011.5979697

52. David Silvera Tawil, David Rye, Manuchehr Soleimani, and Mari Velonaki. 2015. Electrical Impedance Tomography for Artificial Sensitive Robotic Skin : A Review. IEEE Sensors Journal, vol. 15, no. 4, 2001-2016 http://doi.org/10.1109/JSEN.2014.2375346

53. Marko Vauhkonen, W.R.B. Lionheart, Lasse M Heikkinen, P.J. Vauhkonen and Jari P Kaipio. A MATLAB package for the EIDORS project to reconstruct two-dimensional EIT images. Physiological Measurement 22.1 107–111 http://doi.org/10.1088/0967-3334/22/1/314

54. Andrew D. Wilson and Hrvoje Benko. 2010. Combining multiple depth cameras and projectors for interactions on, above and between surfaces. In Proceedings of the 23nd annual ACM symposium on User interface software and technology (UIST '10). ACM, New York, NY, USA, 273-282. http://doi.org/10.1145/1866029.1866073

55. Andrew D. Wilson. 2005. PlayAnywhere: a compact interactive tabletop projection-vision system. In Proceedings of the 18th annual ACM symposium on User interface software and technology (UIST '05). ACM, New York, NY, USA, 83-92. http://doi.org/10.1145/1095034.1095047

56. Karl Willis, Eric Brockmeyer, Scott Hudson, and Ivan Poupyrev. 2012. Printed optics: 3D printing of embedded optical elements for interactive devices. In Proceedings of the 25th annual ACM symposium on User interface software and technology (UIST '12). ACM, New York, NY, USA, 589-598. http://doi.org/10.1145/2380116.2380190

57. Raphael Wimmer and Patrick Baudisch. 2011. Modular and deformable touch-sensitive surfaces based on time domain reflectometry. In Proceedings of the 24th annual ACM symposium on User interface software and technology (UIST '11). ACM, New York, NY, USA, 517-526. http://doi.org/10.1145/2047196.2047264

58. Robert Xiao, Chris Harrison, and Scott E. Hudson. 2013. WorldKit: rapid and easy creation of ad-hoc interactive applications on everyday surfaces. In CHI '13 Extended Abstracts on Human Factors in Computing

Systems (CHI EA '13). ACM, New York, NY, USA, 2889-2890. http://doi.org/10.1145/2468356.2479563

59. Robert Xiao, Greg Lew, James Marsanico, Divya Hariharan, Scott Hudson, and Chris Harrison. 2014. Toffee: enabling ad hoc, around-device interaction with acoustic time-of-arrival correlation. In Proceedings of the 16th international conference on Human-computer interaction with mobile devices & services (MobileHCI '14). ACM, New York, NY, USA, 67-76. http://doi.org/10.1145/2628363.2628383

60. Zen ToolWorks Inc: http://www.zentoolworks.com

61. Thomas G. Zimmerman, Joshua R. Smith, Joseph A. Paradiso, David Allport, and Neil Gershenfeld. 1995. Applying electric field sensing to human-computer interfaces. In Proceedings of the SIGCHI Conference on Human Factors in Computing Systems (CHI '95).

ACM, New York, NY, USA, 280-287. http://doi.org/10.1145/223904.223940

62. Yang Zhang and Chris Harrison. 2015. Tomo: Wearable, Low-Cost Electrical Impedance Tomography for Hand Gesture Recognition. In Proceedings of the 28th Annual ACM Symposium on User Interface Software & Technology (UIST '15). ACM, New York, NY, USA, 167-173. http://doi.org/10.1145/2807442.2807480

63. Yang Zhang, Robert Xiao, and Chris Harrison. 2016. Advancing Hand Gesture Recognition with High Resolution Electrical Impedance Tomography. In Proceedings of the 29th Annual Symposium on User Interface Software and Technology (UIST '16). ACM, New York, NY, USA, 843-850. http://doi.org/10.1145/2984511.2984574